Comparison of Stiff Chemistry Solvers for Air Quality Modeling

ARTICLE *in* ENVIRONMENTAL SCIENCE AND TECHNOLOGY · OCTOBER 1994

Impact Factor: 5.33 · DOI: 10.1021/es00060a019 · Source: PubMed

3 AUTHORS, INCLUDING:

David Chock
University of Michigan
80 PUBLICATIONS **1,256** CITATIONS
SEE PROFILE

Pu Sun
General Motors Company
17 PUBLICATIONS **139** CITATIONS
SEE PROFILE

Environ. Sci. Technol. 1994, 28, 1882–1892

Comparison of Stiff Chemistry Solvers for Air Quality Modeling

David P. Chock,* Sandra L. Winkler, and Pu Sun†

Ford Research Laboratory, Ford Motor Company, P.O. Box 2053, MD-3083, Dearborn, Michigan 48121

Four fast solvers and their variations are compared in terms of the accuracy of the solutions and computation time when they are used to solve a system of stiff ordinary differential equations describing the carbon bond IV mechanism in air quality modeling. The solvers are the Urban Airshed Model (UAM) solver, the quasi-steady-state assumption (QSSA), and the Hybrid solvers, each with an additional version employing the steady-state algorithm of the UAM solver, and the new implicit–explicit hybrid (IEH) solver under two different sets of error tolerance. The solvers were run for one 6-min time step under 256 different initial conditions for both daytime and nighttime. In terms of accuracy, the IEH solvers are the most accurate, while the QSSA solver is the least accurate. In terms of computation time, QSSA and QSSA with UAM steady state are the fastest, while UAM is the slowest for daytime integration and widely variable for nighttime integration. The more tolerant version of IEH (IEH26) and the Hybrid solver coupled with UAM steady state are fast, but the former is more accurate under all tested conditions, assumes only one steady-state species (O1D), conserves the nitrogen mass, and is applicable to other stiff chemical systems. Accordingly, IEH26 should be an excellent candidate as a fast and accurate chemistry solver in air quality modeling, combustion, and other reactive flow systems.

Introduction

In a three-dimensional (3D) air quality model, both transport and chemistry of air pollutants are simulated. A time-splitting scheme is generally used to integrate the transport and chemistry steps in an alternating sequence. Depending on the method of choice, the chemistry step has to be re-initialized at every one or two time steps (Δt, typically 4–10 min). The atmospheric chemistry involves several tens of chemical species and some 80 to more than 100 chemical reactions with a very wide range of reaction rate constants. Solving the resulting stiff chemical kinetic equations for the tens of chemical species for each time step and for each of the grid cells in the model is usually the most time-consuming step in three-dimensional air quality modeling. Using the accurate, standard methods such as the Livermore Solver for Ordinary Differential Equations (*1*) (LSODE) would require an unrealistically long computation time to complete a multiday air quality simulation with today's computers. Fast solvers are presently used for these stiff chemical systems to reduce computation time, often with a sacrifice in accuracy. The most frequently used fast solvers in air quality modeling are the quasi-steady-state approximation (QSSA) scheme (*2*) and the Hybrid scheme (*3*). The Urban Airshed Model (*4*) (UAM) uses a fast solver of its own. More recently, a new solver, an implicit–explicit hybrid (IEH) scheme, has been developed (*5*). Comparison of the QSSA and Hybrid schemes were recently carried out by Odman *et al.* (*6*) using a limited number of initial conditions and an integrating period of up to 3 days. This paper compares the performance of the above four solvers, each with one or two variations, in terms of their computation time and accuracy of the results. Rather than running the solvers for a long time period, only one time step will be used in a similar fashion as in 3D simulation. In addition, a wide range of initial conditions will be applied to assess the robustness of the solvers. Such a test allows one to explore, without the interference of extraneous factors, the performance of the solvers in greater detail under a wide range of conditions encountered in the full air quality model. Adoption of the IEH solver in the full UAM will be reported elsewhere. The solvers, test cases, and results are described in sections 2–4, respectively. Section 5 gives the conclusion.

Description of Solvers

The system of stiff ordinary differential equations can be written as

$$\frac{d\boldsymbol{C}}{dt} = \boldsymbol{f}(\boldsymbol{C},t) = \boldsymbol{P} - \boldsymbol{L}\boldsymbol{C} \quad (1)$$

where $\boldsymbol{C}(t)$ is the concentration vector at time t. In all the schemes presented here except IEH, the second line of eq 1 is assumed where $\boldsymbol{P}$ and $\boldsymbol{LC}$ represent the production and loss terms, $\boldsymbol{L}$ being a diagonal matrix. In particular, for component or species i, both P_i and L_i do not contain C_i explicitly. L_i has the dimension of (time)$^{-1}$ and is often written as $1/\tau_i$ where τ_i represents the characteristic decay time for C_i. At steady state or equilibrium, τ_i equals the growth time scale, C_i/P_i, and the reaction time scale, C_i/f_i, for C_i is zero. The choice of the integration step, h, relative to the characteristic times or time scales is critical in determining the accuracy of the fast solvers.

In the QSSA scheme, h is selected as input and kept constant within the scheme. No self-adjustment mechanism for h is incorporated. If h/τ_i is large, say, >10, then a steady state for C_i is assumed. If h/τ_i is small, say, <0.01, then C_i is determined by the forward Euler method. If h/τ_i is somewhere in between, then an analytic formula for C_i is used. This analytic formula is the exact solution to the second form of eq 1 with P_i and L_i assumed constant. The scheme saves time by not using convergence criteria and not adjusting h internally. Thus, tracking the relative changes of C_i after each integration step becomes unnecessary. But this fact also contributes to the difficulty in assuring accuracy and stability of the scheme. Hesstvedt *et al.* (*2*) recommend an integration step of 30 s for air pollution chemistry. Shieh *et al.* (*7*) used an integration step of 30 s for daytime, 60 s for nighttime, but 12 s during sunrise and sunset to maintain stability of the scheme.

† Also at Institute for Mathematics and Its Applications, University of Minnesota, Minneapolis, MN 55455, through June 1994.

0013-936X/94/0928-1882$04.50/0

Table 1. Initial Concentrations (ppm)[a]

	low	high	fixed					
NO	2×10^{-3}	6×10^{-2}	HONO	1×10^{-4}	OH	3.5×10^{-8}	CRES	1×10^{-5}
NO_2	2×10^{-3}	6×10^{-2}	H_2O_2	1×10^{-5}	C_2O_3	8.7×10^{-9}	PNA	1×10^{-5}
O_3	2×10^{-3}	3×10^{-1}	MGLY	1×10^{-3}	TO_2	6.6×10^{-9}	O1D	1.6×10^{-12}
OLE	1×10^{-3}	3×10^{-2}	CO	5×10^{0}	CRO	1.3×10^{-11}	NO_3	1×10^{-5}
TOL	1×10^{-3}	1×10^{-2}	ETH	1×10^{-2}	HNO_3	1×10^{-5}	HO_2	1.7×10^{-7}
XYL	3×10^{-4}	1×10^{-2}	ISOP	1×10^{-2}	PAN	1×10^{-2}	ROR	5.9×10^{-11}
FORM	1×10^{-3}	1×10^{-2}	O	1.8×10^{-9}	OPEN	1×10^{-5}	XO_2	1.1×10^{-7}
ALD2	1×10^{-3}	2×10^{-2}	N_2O_5	8.1×10^{-9}	PAR	5×10^{-1}	XO_2N	4.6×10^{-8}

[a] Combining the low and high concentrations of species in the low and high columns generates a total of 256 initial conditions.

Odman *et al.* (*6*) show the improvement in accuracy as h is reduced to 5 s for photochemical simulation. Reducing h reduces not only the errors associated with the choice of integration methods in the three h/τ_i regimes but also the potential problem of using only the characteristic decay time to classify the integration regimes. In fact, ignoring the growth time scale that may turn out to be very small is likely to be the main reason for inaccuracy and instability in this scheme.

In the Hybrid scheme, the initial integration step is determined internally as a fraction of the minimum of the reaction time scales of all the C_i at time t:

$$h = \epsilon \min\left(\frac{C_i}{f_i}\right) \tag{2}$$

where ϵ is a scale factor chosen to be comparable to the relative error or convergence criterion for the iterations in the predictor–corrector integration. If h/τ_i is greater than, say, 1, then the corresponding equation for C_i is considered stiff at time t. Otherwise it is normal or non-stiff. A simple first-order predictor–second-order corrector scheme is used for the non-stiff equations, and a stable asymptotic predictor–corrector scheme is used for the stiff equations. The asymptotic formula (*3*) yields an accurate solution when C_i approaches equilibrium while both the characteristic decay time and the growth time scale are small. Within each integration step, both the stiff and non-stiff corrector steps are repeated by iteration until a given convergence criterion is met for all the species concentrations. Success or failure in meeting the criterion will lead to a lengthening of the integration step after the iteration or a shortening of the integration step during the iteration. This scheme uses a self-adjusting h and is clearly stable. It is expected to have improved accuracy but longer execution time compared to the QSSA scheme.

The UAM solver is not well-documented. Tracing the source code is also difficult. It is a scheme hard-wired to the carbon bond IV (denoted CB4) mechanism (*8*). The scheme uses a modified Crank–Nicolson algorithm expressed in the form of a predictor–corrector procedure for

Table 2. Average |RE| over All Initial Conditions (Excluding Cases below Threshold) for Daytime

species	threshold	no. of cases below threshold	solver						
			UAM	QSSA	QSSA + SS	Hybrid	Hybrid + SS	1EH37	1EH26
NO	1.0×10^{-5}	0	1.456×10^{-2}	2.263×10^{-1}	8.428×10^{-2}	2.274×10^{-1}	8.191×10^{-3}	1.977×10^{-4}	1.592×10^{-3}
NO_2	1.0×10^{-5}	0	1.037×10^{-2}	4.920×10^{-1}	1.236×10^{-1}	1.664×10^{-1}	1.055×10^{-2}	1.842×10^{-4}	1.522×10^{-3}
O_3	1.0×10^{-5}	0	1.155×10^{-2}	1.759×10^{0}	8.659×10^{-2}	1.420×10^{-1}	1.060×10^{-2}	2.672×10^{-4}	1.151×10^{-3}
PNA	1.0×10^{-7}	0	1.487×10^{-1}	9.760×10^{-1}	3.285×10^{-1}	9.959×10^{-1}	1.429×10^{-1}	8.479×10^{-4}	2.489×10^{-3}
O1D	1.0×10^{-18}	0	1.735×10^{-1}	1.760×10^{0}	1.120×10^{-1}	8.139×10^{-1}	1.061×10^{-2}	1.618×10^{-1}	1.628×10^{-1}
O	1.0×10^{-13}	0	8.806×10^{-3}	5.924×10^{-1}	1.347×10^{-1}	6.562×10^{-1}	8.353×10^{-3}	1.664×10^{-4}	1.301×10^{-3}
NO_3	1.0×10^{-9}	32	2.061×10^{-2}	1.751×10^{0}	1.319×10^{-1}	1.831×10^{-1}	8.671×10^{-3}	6.435×10^{-4}	4.473×10^{-3}
N_2O_5	1.0×10^{-7}	64	8.821×10^{-3}	1.168×10^{0}	8.392×10^{-2}	7.424×10^{-2}	6.323×10^{-3}	8.357×10^{-4}	3.454×10^{-3}
HO_2	1.0×10^{-7}	0	5.452×10^{-2}	9.877×10^{-1}	3.465×10^{-1}	9.956×10^{-1}	3.704×10^{-2}	7.073×10^{-4}	1.794×10^{-3}
OH	1.0×10^{-11}	0	6.175×10^{-2}	8.658×10^{-1}	3.101×10^{-1}	9.595×10^{-1}	3.220×10^{-2}	7.576×10^{-4}	1.999×10^{-3}
ROR	1.0×10^{-14}	0	6.171×10^{-2}	8.624×10^{-1}	3.094×10^{-1}	9.621×10^{-1}	3.218×10^{-2}	7.546×10^{-4}	1.999×10^{-3}
C_2O_3	1.0×10^{-10}	0	4.311×10^{-2}	9.000×10^{-1}	3.680×10^{-1}	9.650×10^{-1}	2.932×10^{-2}	8.302×10^{-4}	2.871×10^{-3}
XO_2	1.0×10^{-7}	0	6.169×10^{-2}	7.823×10^{-1}	2.863×10^{-1}	9.216×10^{-1}	3.988×10^{-2}	7.457×10^{-4}	2.195×10^{-3}
TO_2	1.0×10^{-11}	0	6.206×10^{-2}	8.429×10^{-1}	3.108×10^{-1}	9.636×10^{-1}	3.298×10^{-2}	7.352×10^{-4}	1.913×10^{-3}
XO_2N	1.0×10^{-7}	0	6.505×10^{-2}	7.792×10^{-1}	1.844×10^{-1}	7.295×10^{-1}	5.465×10^{-2}	8.042×10^{-4}	1.948×10^{-3}
CRO	1.0×10^{-10}	40	6.689×10^{-2}	2.482×10^{0}	5.227×10^{-1}	8.228×10^{-1}	4.444×10^{-2}	1.102×10^{-2}	2.042×10^{-2}
HONO	1.0×10^{-7}	0	1.715×10^{-2}	7.275×10^{-1}	4.899×10^{-1}	3.365×10^{-1}	1.245×10^{-2}	1.086×10^{-3}	3.481×10^{-3}
HNO_3	1.0×10^{-6}	0	8.642×10^{-2}	5.022×10^{0}	5.528×10^{-1}	8.176×10^{-1}	2.869×10^{-2}	1.888×10^{-3}	4.404×10^{-3}
H_2O_2	1.0×10^{-7}	0	7.630×10^{-2}	2.746×10^{-1}	2.131×10^{-1}	2.717×10^{-1}	2.571×10^{-2}	6.308×10^{-4}	1.859×10^{-3}
FORM	1.0×10^{-4}	0	1.634×10^{-2}	8.152×10^{-1}	1.949×10^{-1}	2.455×10^{-1}	7.973×10^{-3}	3.937×10^{-4}	1.281×10^{-3}
ALD2	1.0×10^{-5}	0	1.074×10^{-2}	6.340×10^{-1}	1.366×10^{-1}	1.584×10^{-1}	5.888×10^{-3}	2.879×10^{-4}	8.831×10^{-4}
PAN	1.0×10^{-7}	0	5.393×10^{-2}	7.104×10^{-1}	5.736×10^{-1}	9.034×10^{-1}	2.746×10^{-2}	1.132×10^{-3}	3.151×10^{-3}
MGLY	1.0×10^{-6}	0	1.429×10^{-2}	7.618×10^{-1}	8.227×10^{-2}	2.097×10^{-1}	7.103×10^{-3}	3.516×10^{-4}	1.123×10^{-3}
OPEN	1.0×10^{-8}	0	2.216×10^{-2}	1.429×10^{0}	2.201×10^{-1}	3.510×10^{-1}	1.042×10^{-2}	4.866×10^{-4}	1.970×10^{-3}
CO	1.0×10^{-3}	0	8.209×10^{-6}	4.279×10^{-4}	3.504×10^{-5}	1.192×10^{-4}	4.170×10^{-6}	3.188×10^{-7}	6.387×10^{-7}
PAR	1.0×10^{-5}	0	1.016×10^{-4}	5.543×10^{-3}	1.409×10^{-3}	1.593×10^{-3}	6.038×10^{-5}	2.972×10^{-6}	8.678×10^{-6}
OLE	1.0×10^{-5}	0	1.145×10^{-3}	6.138×10^{-2}	2.213×10^{-2}	1.664×10^{-2}	5.882×10^{-4}	3.150×10^{-5}	9.235×10^{-5}
ETH	1.0×10^{-5}	0	3.269×10^{-3}	1.835×10^{-1}	3.313×10^{-2}	4.779×10^{-2}	1.639×10^{-3}	8.642×10^{-5}	2.669×10^{-4}
TOL	1.0×10^{-5}	0	2.504×10^{-4}	1.333×10^{-2}	2.337×10^{-3}	3.645×10^{-3}	1.295×10^{-4}	6.708×10^{-6}	1.972×10^{-5}
XYL	1.0×10^{-5}	0	1.021×10^{-3}	5.304×10^{-2}	9.534×10^{-3}	1.491×10^{-2}	5.261×10^{-4}	2.766×10^{-5}	8.133×10^{-5}
CRES	1.0×10^{-8}	0	5.303×10^{-2}	2.208×10^{0}	4.317×10^{-1}	6.755×10^{-1}	2.352×10^{-3}	1.444×10^{-3}	4.022×10^{-3}
ISOP	1.0×10^{-7}	0	3.973×10^{-3}	1.990×10^{-1}	5.255×10^{-2}	6.106×10^{-2}	2.052×10^{-3}	1.114×10^{-4}	3.415×10^{-4}

Table 3. Average |RE| over All Initial Conditions (Excluding Cases below Threshold) for Nighttime

species	threshold	no. of cases below threshold	solver						
			UAM	QSSA	QSSA + SS	Hybrid	Hybrid + SS	IEH37	IEH26
NO	1.0×10^{-5}	128	5.050×10^{-1}	9.435×10^{-1}	5.039×10^{-1}	6.023×10^{-1}	5.055×10^{-1}	1.229×10^{-3}	1.434×10^{-2}
NO_2	1.0×10^{-5}	0	6.012×10^{-2}	1.370×10^{0}	1.056×10^{-1}	7.604×10^{-2}	9.597×10^{-2}	7.828×10^{-5}	1.031×10^{-3}
O_3	1.0×10^{-5}	64	3.348×10^{-1}	8.658×10^{0}	3.439×10^{-1}	1.486×10^{-2}	3.348×10^{-1}	4.842×10^{-4}	5.043×10^{-3}
PNA	1.0×10^{-7}	28	9.051×10^{-1}	9.813×10^{-1}	1.083×10^{0}	9.963×10^{-1}	6.383×10^{-1}	1.698×10^{-3}	8.399×10^{-3}
O1D	1.0×10^{-18}	64	6.442×10^{4}	8.672×10^{0}	6.442×10^{4}	1.132×10^{0}	1.000×10^{0}	1.620×10^{-1}	1.674×10^{-1}
O	1.0×10^{-13}	128	1.152×10^{2}	1.659×10^{-1}	1.152×10^{2}	1.100×10^{0}	1.000×10^{0}	7.928×10^{-6}	9.431×10^{-5}
NO_3	1.0×10^{-9}	64	4.244×10^{-1}	3.213×10^{1}	7.013×10^{-1}	1.559×10^{-1}	4.534×10^{-1}	1.780×10^{-3}	2.231×10^{-2}
N_2O_5	1.0×10^{-7}	96	2.915×10^{-1}	1.040×10^{1}	6.427×10^{-1}	1.133×10^{-1}	3.275×10^{-1}	1.984×10^{-3}	1.631×10^{-2}
HO_2	1.0×10^{-7}	36	4.843×10^{-1}	9.959×10^{-1}	8.491×10^{-1}	9.981×10^{-1}	6.172×10^{-1}	1.758×10^{-3}	7.923×10^{-3}
OH	1.0×10^{-11}	0	7.465×10^{-1}	6.992×10^{-1}	8.083×10^{-1}	9.222×10^{-1}	7.322×10^{-1}	1.421×10^{-3}	1.092×10^{-2}
ROR	1.0×10^{-14}	0	6.524×10^{2}	7.002×10^{-1}	2.027×10^{2}	9.017×10^{-1}	2.835×10^{2}	1.421×10^{-3}	1.092×10^{-2}
C_2O_3	1.0×10^{-10}	0	5.819×10^{-1}	8.482×10^{-1}	7.268×10^{-1}	9.704×10^{-1}	5.964×10^{-1}	1.284×10^{-3}	1.063×10^{-2}
XO_2	1.0×10^{-7}	52	4.313×10^{-1}	1.182×10^{1}	4.688×10^{-1}	5.695×10^{-1}	4.560×10^{-1}	1.893×10^{-3}	8.491×10^{-3}
TO_2	1.0×10^{-11}	0	5.790×10^{0}	6.974×10^{-1}	5.684×10^{0}	9.157×10^{-1}	9.810×10^{-1}	1.399×10^{-3}	1.041×10^{-2}
XO_2N	1.0×10^{-7}	48	9.900×10^{-1}	4.919×10^{1}	9.875×10^{-1}	3.637×10^{-1}	9.978×10^{-1}	1.938×10^{-3}	1.005×10^{-2}
CRO	1.0×10^{-10}	101	9.348×10^{-1}	6.719×10^{1}	5.376×10^{0}	8.308×10^{-1}	1.715×10^{0}	3.735×10^{0}	6.439×10^{0}
HONO	1.0×10^{-7}	0	5.414×10^{-2}	1.361×10^{0}	5.097×10^{-2}	6.799×10^{-2}	5.872×10^{-2}	5.899×10^{-4}	1.240×10^{-3}
HNO_3	1.0×10^{-6}	0	3.467×10^{-1}	1.914×10^{1}	6.388×10^{-1}	6.194×10^{-1}	3.510×10^{-1}	4.710×10^{-3}	2.261×10^{-2}
H_2O_2	1.0×10^{-7}	0	1.658×10^{-1}	3.948×10^{-1}	3.763×10^{-1}	3.924×10^{-1}	2.054×10^{-1}	1.523×10^{-3}	6.479×10^{-3}
FORM	1.0×10^{-5}	0	3.376×10^{-2}	1.597×10^{0}	1.247×10^{-1}	4.280×10^{-2}	3.508×10^{-2}	3.361×10^{-4}	2.712×10^{-3}
ALD2	1.0×10^{-5}	0	2.961×10^{-2}	1.030×10^{0}	8.350×10^{-2}	3.175×10^{-2}	3.051×10^{-2}	2.309×10^{-4}	2.324×10^{-3}
PAN	1.0×10^{-7}	0	3.938×10^{-1}	1.655×10^{0}	6.676×10^{-1}	7.439×10^{-1}	4.242×10^{-1}	1.778×10^{-3}	1.046×10^{-2}
MGLY	1.0×10^{-6}	0	2.996×10^{-2}	1.133×10^{0}	5.266×10^{-2}	3.892×10^{-2}	3.154×10^{-2}	2.371×10^{-4}	1.865×10^{-3}
OPEN	1.0×10^{-8}	0	6.080×10^{-2}	1.333×10^{0}	6.185×10^{-2}	6.917×10^{-2}	6.526×10^{-2}	4.588×10^{-4}	1.474×10^{-3}
CO	1.0×10^{-3}	0	9.234×10^{-6}	5.535×10^{-4}	1.692×10^{-5}	1.947×10^{-5}	9.067×10^{-6}	2.357×10^{-7}	9.776×10^{-7}
PAR	1.0×10^{-5}	0	2.195×10^{-4}	6.668×10^{-3}	7.137×10^{-4}	2.379×10^{-4}	2.304×10^{-4}	1.666×10^{-6}	1.425×10^{-5}
OLE	1.0×10^{-5}	0	3.194×10^{-3}	7.016×10^{-2}	1.898×10^{-2}	2.370×10^{-3}	3.210×10^{-3}	2.099×10^{-5}	1.721×10^{-4}
ETH	1.0×10^{-5}	0	5.995×10^{-3}	2.315×10^{-1}	9.964×10^{-3}	7.849×10^{-3}	6.278×10^{-3}	4.897×10^{-5}	3.763×10^{-4}
TOL	1.0×10^{-5}	0	4.369×10^{-4}	1.601×10^{-2}	5.662×10^{-4}	5.729×10^{-4}	4.655×10^{-4}	3.446×10^{-6}	2.710×10^{-5}
XYL	1.0×10^{-5}	0	1.778×10^{-3}	6.345×10^{-2}	2.303×10^{-3}	2.330×10^{-3}	1.894×10^{-3}	1.392×10^{-5}	1.100×10^{-4}
CRES	1.0×10^{-8}	4	4.992×10^{0}	1.057×10^{1}	5.744×10^{0}	5.456×10^{-1}	2.707×10^{0}	2.591×10^{0}	4.003×10^{0}
ISOP	1.0×10^{-7}	0	6.666×10^{-2}	1.859×10^{-1}	2.010×10^{-1}	1.119×10^{-2}	5.100×10^{-2}	9.703×10^{-4}	3.866×10^{-3}

non-steady-state species concentrations. The calculations for the steady-state species concentrations are quite elaborate and contain assumptions specific to the mechanism. All free radicals plus NO_3 and N_2O_5, a total of 12 (shown from row 5 to row 16 in Table 2), are considered steady-state species. For nighttime, O_3, NO, and NO_3 are assumed to react instantaneously. But to assure stability, two separate assumptions for nighttime chemistry are required, one of which is used only if the concentrations of both NO and O_3 are less than 10^{-4} ppm. The initial h is Δt but not greater than 6 min; the scheme adjusts it based on a given convergence criterion.

The three solvers above all avoid inverting the Jacobian matrix which is needed in the Newton iteration procedure for the commonly used backward-differentiation formulas methods such as LSODE. This allows the solvers to be fast, but at a price of a potential loss of accuracy. Also, as h/τ_i becomes large (>10), QSSA invokes the steady-state assumption while the Hybrid scheme yields the steady-state solution asymptotically. To reduce the computation time further, many free-radical species are explicitly assumed to be in steady state. Use of the steady-state assumption coupled with non-steady-state computation can cause the solvers not to conserve mass accurately. An external forcing of mass conservation tends to have an unpredictable impact on the solution. In addition, the steady-state assumption may lead to a set of nonlinear algebraic equations which may not be straightforward to solve, especially when multiple real solutions exist.

The IEH scheme attempts to preserve the accuracy of the backward-differentiation formulas methods while reducing the computation time by reducing the size of the Jacobian matrix. This is done by separating the species concentrations into fast-reacting (stiff) and slow-reacting (non-stiff) groups, solving the former implicitly and the latter explicitly. The fast-reacting species include free radicals and species that display abrupt changes in concentrations in the initial fraction of a time step. Oxides of nitrogen and ozone are included also to assure their accuracy. The slow-reacting species include all organic compounds, hydrogen peroxide, and nitrous and nitric acids (5). The classification can be greatly facilitated by an initial investigation of the temporal behavior of all the species using a very small time step in a full-scale LSODE application. The temporal behavior of the species concentrations generally does not change under a wide range of initial conditions. The IEH scheme can be adopted for any combination of fast- and slow-reacting species classifications. Clearly, increasing the number of fast-reacting species will assure greater accuracy in the solution but also a longer computation time. Equation 1 is now expressed as follows:

$$\frac{d\boldsymbol{C}_F}{dt} = \boldsymbol{f}_F(\boldsymbol{C}_F, \boldsymbol{C}_S, t)$$

$$\frac{d\boldsymbol{C}_S}{dt} = \boldsymbol{f}_S(\boldsymbol{C}_F, \boldsymbol{C}_S, t) \qquad (3)$$

where $\boldsymbol{C}_F$ and $\boldsymbol{C}_S$ are the fast-reacting and slow-reacting species concentrations, respectively. Note that the IEH scheme is not restricted to the second form of eq 1. With eq 3 replacing eq 1, the size of the Jacobian matrix for the stiff equations (equations for $\boldsymbol{C}_F$) is substantially reduced compared to the original equations. Because the backward-differentiation formulas method is used to solve the

Table 4. Fraction of All Initial Conditions (Excluding Cases below Threshold) with |RE| <25% for Daytime

species	threshold	no. of cases below threshold	solver						
			UAM	QSSA	QSSA + SS	Hybrid	Hybrid + SS	IEH37	IEH26
NO	1.0×10^{-5}	0	1.000	0.516	0.922	0.805	1.000	1.000	1.000
NO_2	1.0×10^{-5}	0	1.000	0.750	0.785	0.750	1.000	1.000	1.000
O_3	1.0×10^{-15}	0	1.000	0.391	0.809	0.750	1.000	1.000	1.000
PNA	1.0×10^{-7}	0	0.898	0.000	0.469	0.000	0.875	1.000	1.000
O1D	1.0×10^{-18}	0	1.000	0.391	0.750	0.156	1.000	1.000	1.000
O	1.0×10^{-13}	0	1.000	0.625	0.762	0.230	1.000	1.000	1.000
NO_3	1.0×10^{-9}	32	1.000	0.424	0.897	0.857	1.000	1.000	1.000
N_2O_5	1.0×10^{-7}	64	1.000	0.469	0.891	1.000	1.000	1.000	1.000
HO_2	1.0×10^{-7}	0	1.000	0.000	0.422	0.000	1.000	1.000	1.000
OH	1.0×10^{-11}	0	1.000	0.000	0.520	0.000	1.000	1.000	1.000
ROR	1.0×10^{-14}	0	1.000	0.000	0.520	0.000	1.000	1.000	1.000
C_2O_3	1.0×10^{-10}	0	1.000	0.000	0.375	0.000	1.000	1.000	1.000
OX_2	1.0×10^{-7}	0	1.000	0.000	0.508	0.000	1.000	1.000	1.000
TO_2	1.0×10^{-11}	0	1.000	0.000	0.520	0.000	1.000	1.000	1.000
XO_2N	1.0×10^{-7}	0	0.965	0.078	5.754	0.000	0.965	1.000	1.000
CRO	1.0×10^{-10}	40	1.000	0.000	0.144	0.000	1.000	1.000	1.000
HONO	1.0×10^{-7}	0	1.000	0.488	0.406	0.500	1.000	1.000	1.000
HNO_3	1.0×10^{-6}	0	0.965	0.000	0.180	0.000	1.000	1.000	1.000
H_2O_2	1.0×10^{-7}	0	0.938	0.625	0.641	0.625	1.000	1.000	1.000
FORM	1.0×10^{-5}	0	1.000	0.332	0.684	0.555	1.000	1.000	1.000
ALD2	1.0×10^{-5}	0	1.000	0.500	0.766	0.691	1.000	1.000	1.000
PAN	1.0×10^{-7}	0	1.000	0.074	0.039	0.000	1.000	1.000	1.000
MGLY	1.0×10^{-6}	0	1.000	0.000	0.969	0.727	1.000	1.000	1.000
OPEN	1.0×10^{-8}	0	1.000	0.172	0.586	0.410	1.000	1.000	1.000
CO	1.0×10^{-3}	0	1.000	1.000	1.000	1.000	1.000	1.000	1.000
PAR	1.0×10^{-5}	0	1.000	1.000	1.000	1.000	1.000	1.000	1.000
OLE	1.0×10^{-5}	0	1.000	1.000	1.000	1.000	1.000	1.000	1.000
ETH	1.0×10^{-5}	0	1.000	0.969	1.000	1.000	1.000	1.000	1.000
TOL	1.0×10^{-5}	0	1.000	1.000	1.000	1.000	1.000	1.000	1.000
XYL	1.0×10^{-5}	0	1.000	1.000	1.000	1.000	1.000	1.000	1.000
CRES	1.0×10^{-8}	0	1.000	0.039	0.195	0.082	1.000	1.000	1.000
ISOP	1.0×10^{-7}	0	1.000	0.922	1.000	1.000	1.000	1.000	1.000

equations for C_F, the scheme should be highly accurate and mass conserving.

Test Cases

We compare the different solvers using the CB4 mechanism. This mechanism is the only choice if the UAM solver is to be compared with other solvers because the UAM solver, together with its treatment of steady-state species, is designed specifically for CB4 and not readily transportable to other mechanisms. The version of CB4 is identical to that in UAM version 6.20, but with the reaction rates for $XO_2 + HO_2$, $C_2O_3 + NO$, and $C_2O_3 + NO_2$ and the thermal decomposition of PAN updated (*9*). The mechanism contains 38 species (including free radicals) and 86 reactions. For the IEH, QSSA, and Hybrid solvers not using the UAM steady-state assumptions, reaction 87 for MTBE + OH is also included but NXOY, which is an extraneous accounting parameter for some oxides of nitrogen species needed only in the UAM solver for steady-state calculations, is not included. Inclusion of MTBE will slow down the affected solvers, but most likely only slightly. Our comparison covers both the daytime and nighttime conditions. For the daytime case, the photolysis rate constants are set at their maximum values corresponding to the noontime condition in Los Angeles. For the nighttime case, the photolysis rates are set equal to zero. At night, even though the stiffness of the Jacobian will be reduced, sharp variations, such as a sharp drop to essentially zero in some species concentrations, often occur. For all cases, the temperature is set at 310 K.

Since a solver may perform differently under different initial conditions, we establish for both daytime and nighttime runs 256 initial conditions by combining either a low or a high concentration from each of the eight chemical species while holding other species concentrations constant. Table 1 shows the initial concentrations used in the present study. They are identical to those used in Sun *et al.* (*5*). The range of the initial concentration ratios of total organic species to NO_x (NO + NO_2) is 4.9–208 ppm C/ppm. The initial concentrations of five of the 38 species (MEOH, ETOH, NTR, SO_2, and SULF) are set equal to zero and do not appear in Table 1. NTR is a product and chain terminator. The initial condition of MTBE is also set equal to zero for solvers that are applied to the 87-reaction set. Not all of the 256 initial conditions are realistic for both daytime and nighttime conditions. For example, it would be uncommon to observe an O_3 concentration of, say, 0.2–0.3 ppm (the high O_3 initial conditions) late at night or early in the morning. However, it is desirable to see whether a solver is accurate under a wide range of conditions. Our time integration is performed for one Δt, which is set at 6 min. This Δt is typical of the time step used in 3D air quality modeling. It is more meaningful and stressful to test the solvers for only one time step under a wide range of initial conditions than for a long period but under a very limited number of initial conditions. This is because the initial condition for the chemistry step is updated at every time step or two anyway in 3D modeling to incorporate the effect of transport, emissions, etc. But more importantly, because the concentrations of the stiff species have to be quickly adjusted to approach their asymptotic solutions within the very first tiny fraction of the time step, a brand new initial condition is likely to require more substantial adjustments

Table 5. Fraction of All Initial Conditions (Excluding Cases below Threshold) with |RE| <25% for Nighttime

species	threshold	no. of cases below threshold	solver						
			UAM	QSSA	QSSA + SS	Hybrid	Hybrid + SS	IEH37	IEH26
NO	1.0×10^{-5}	128	0.500	0.000	0.500	0.641	0.500	1.000	1.000
NO_2	1.0×10^{-5}	0	0.922	0.750	0.891	0.906	0.891	1.000	1.000
O_3	1.0×10^{-5}	64	0.667	0.667	0.667	1.000	0.667	1.000	1.000
PNA	1.0×10^{-7}	28	0.430	0.000	0.118	0.000	0.123	1.000	1.000
O1D	1.0×10^{-18}	64	0.000	0.667	0.000	0.000	0.000	1.000	1.000
O	1.0×10^{-13}	128	0.000	1.000	0.000	0.000	0.000	1.000	1.000
NO_3	1.0×10^{-9}	64	0.609	0.042	0.167	0.854	0.500	1.000	1.000
N_2O_5	1.0×10^{-7}	96	0.800	0.056	0.200	0.950	0.600	1.000	1.000
HO_2	1.0×10^{-7}	36	0.423	0.000	0.000	0.000	0.086	1.000	1.000
OH	1.0×10^{-11}	0	0.070	0.000	0.000	0.000	0.000	1.000	1.000
ROR	1.0×10^{-14}	0	0.000	0.000	0.000	0.000	0.000	1.000	1.000
C_2O_3	1.0×10^{-10}	0	0.117	0.043	0.063	0.000	0.031	1.000	1.000
XO_2	1.0×10^{-7}	52	0.627	0.466	0.471	0.314	0.627	1.000	1.000
TO_2	1.0×10^{-11}	0	0.137	0.000	0.137	0.000	0.000	1.000	1.000
XO_2N	1.0×10^{-7}	48	0.000	0.000	0.000	0.615	0.000	1.000	1.000
CRO	1.0×10^{-10}	101	0.000	0.013	0.045	0.000	0.000	0.465	0.452
HONO	1.0×10^{-7}	0	0.938	0.695	0.969	0.906	0.938	1.000	1.000
HNO_3	1.0×10^{-6}	0	0.309	0.000	0.172	0.133	0.375	1.000	1.000
H_2O_2	1.0×10^{-7}	0	0.758	0.465	0.500	0.469	0.512	1.000	1.000
FORM	1.0×10^{-5}	0	1.000	0.012	0.844	1.000	1.000	1.000	1.000
ALD2	1.0×10^{-5}	0	1.000	0.500	0.875	1.000	1.000	1.000	1.000
PAN	1.0×10^{-7}	0	0.266	0.141	0.078	0.094	0.195	1.000	1.000
MGLY	1.0×10^{-6}	0	1.000	0.000	1.000	1.000	1.000	1.000	1.000
OPEN	1.0×10^{-8}	0	0.938	0.563	0.969	0.914	0.922	1.000	1.000
CO	1.0×10^{-3}	0	1.000	1.000	1.000	1.000	1.000	1.000	1.000
PAR	1.0×10^{-5}	0	1.000	1.000	1.000	1.000	1.000	1.000	1.000
OLE	1.0×10^{-5}	0	1.000	1.000	1.000	1.000	1.000	1.000	1.000
ETH	1.0×10^{-5}	0	1.000	0.715	1.000	1.000	1.000	1.000	1.000
TOL	1.0×10^{-5}	0	1.000	1.000	1.000	1.000	1.000	1.000	1.000
XYL	1.0×10^{-5}	0	1.000	1.000	1.000	1.000	1.000	1.000	1.000
CRES	1.0×10^{-8}	4	0.282	0.020	0.306	0.258	0.317	0.655	0.643
ISOP	1.0×10^{-7}	0	1.000	0.781	0.625	1.000	1.000	1.000	1.000

of the stiff species concentrations and, therefore, is more stressful to a solver than one that has already approached a quasi-asymptotic solution from the previous time step.

The scheme against which all other schemes are compared is the LSODE01 described previously (*5*), in double precision, with a relative tolerance (RTOL) of 10^{-7}, an absolute tolerance (ATOL) of 10^{-11} ppm, and an update of the Jacobian at every integral step. No steady state is assumed in LSODE01. All other solvers used are in single precision.

The QSSA routine was extracted from the CALGRID air quality model (*10*). No iterations were performed for species concentrations in equilibrium ($h/\tau_i > 10$) at a given integration step. The routine contains a procedure to improve the nitrogen mass balance of the solver. The procedure sums the nitrogen of all nitrogen-containing species. The resulting lumped-species concentration is solved with the forward Euler scheme (*2*), which conserves nitrogen much better than the equilibrium assumption. The concentration of NO_2 or NO is adjusted to absorb the difference between the Euler-calculated and QSSA-calculated lumped-species concentrations. We chose an integration step of 30 s for both daytime and nighttime. The QSSA solver was run with and without the steady-state assumptions (denoted QSSA + SS and QSSA, respectively). In the case of QSSA + SS, the steady-state calculations are identical to those in the UAM solver for both daytime and nighttime.

The Hybrid solver was extracted from the CIT Photochemical Airshed Model (*11*). Convergence was assumed achieved in the iterative corrector step for both stiff and non-stiff species concentrations when the relative concentration change between two iterations for each species was less than 0.005. Species with iterated concentrations less than 10^{-5} ppm were not subject to the convergence test. No species lumping or redistribution of mass-conservation errors [see, e.g., Odman *et al.* (*6*)] were applied. The Hybrid solver was also run with and without the steady-state assumptions (denoted Hybrid + SS and Hybrid, respectively). The steady-state calculations are again identical to those in the UAM solver.

The UAM solver is identical to that in the model (*4*). The convergence criterion for the iterative corrector for the non-steady-state species is a relative concentration change of 0.02. But for either NO or HNO_3 concentration, the convergence criterion is 10 times greater if the concentration is less than 10^{-4} ppm. The calculations for the steady-state species concentrations are hard-wired to the CB4 mechanism.

The IEH solver used here assumes O1D to be in steady state. Two different versions were run: IEH37 assuming RTOL = 10^{-3}, ATOL = 10^{-7} ppm, and IEH26 assuming RTOL = 10^{-2}, ATOL = 10^{-6} ppm. Both versions update the Jacobian matrix at every 20 integration steps. The double-precision versions of IEH37 and IEH26 were also run, but the results are essentially identical to the single-precision versions. IEH37 is similar to the high-tolerance case in Sun *et al.* (*5*) but with an added steady-state assumption for O1D. Adding the steady-state assumption, relaxing the tolerance, and reducing the frequency of Jacobian update lead to a substantial increase in computation speed.

Results

As in Sun *et al.* (*5*), we define the relative error, RE, at the end of the time step as the concentration difference between a solver and the "exact" solver (LSODE01), divided by the "exact" concentration. For some species, the exact concentrations in some of the 256 cases can be vanishingly small relative to their concentration ranges. This often occurs for nighttime runs and especially for O, N_2O_5, and CRO (See Tables 2 and 3). The RE for this situation may be substantially inflated especially for the less accurate solvers. To minimize the potential distortion, the RE for a given species and initial condition was calculated only when the exact solution was greater than a specified threshold, which was set at about 10^{-3} times the concentration upper bounds for both daytime and nighttime simulations. Tables 2 and 3 show the averages of the absolute values of the relative errors (denoted av|RE|) from each solver for each species concentration over the 256 initial conditions in the daytime and nighttime simulations, respectively. The arrangement of the species in the tables is the same as that in Sun *et al.* (*5*). The top 16 species are the fast-reacting species (according to IEH) while the bottom 16 are the slow-reacting species. Column 2 of the tables gives the threshold values of the exact concentrations below which the |RE| of the corresponding species are excluded from the calculation of the av |RE| for all solvers. Column 3 shows the number of cases in which this condition occurs. As one may expect, very low steady-state species concentrations tend to occur at night according to the exact solutions.

Tables 4 and 5 give for daytime and nighttime, respectively, the fractions of the 256 initial conditions (excluding the cases where the exact concentrations are below the species threshold levels) in which a solver yields a solution within 25% of the exact solutions. For the daytime cases, IEH37 and IEH26 are the most accurate among the solvers, followed by Hybrid + SS and UAM. QSSA + SS does moderately well but poorly for CRO, HNO_3, PAN, and CRES. QSSA and Hybrid are generally not accurate, especially for PNA, HO_2, OH, ROR, C_2O_3, XO_2, TO_2, XO_2N, CRO, HNO_3, PAN, and CRES. In addition, QSSA is also inaccurate for FORM, MGLY, and OPEN. For the nighttime cases, the accuracy of all solvers is somewhat reduced. IEH37 and IEH26 remain the most accurate. They also perform the best for CRO and CRES where all solvers do not do too well. For these two species, the accuracy improves when the tolerance is tightened in the IEH solver (*5*). The other solvers (including Hybrid + SS, UAM, and QSSA + SS) are inaccurate for PNA, HO_2, OH, ROR, C_2O_3, TO_2, XO_2N, CRO, HNO_3, PAN, and CRES. Hybrid performs comparably with Hybrid + SS; it performs especially well for NO_3, N_2O_5 and XO_2N. QSSA is the least accurate. In addition to the species listed for Hybrid + SS etc., it is inaccurate for NO, FORM, and MGLY.

To see how the solvers do under different initial conditions, we show in Figures 1 and 2 for daytime and nighttime conditions, respectively, selected species concentrations after one Δt. These species are chosen either because they are important in air quality or because they can highlight the differences among the solvers. The abscissa of the figures corresponds to the 256 initial conditions, representing all combinations of the low and high initial concentrations of the eight species shown in Table 1. Each initial condition is akin to an eight-digit binary number with the order of the digit from left to right being the same as that of the species from top to bottom in the table. The arrangement of the initial conditions in the abscissa from left to right is identical to an increasing eight-digit binary number where zero and one represent the low and high concentrations of a given species, respectively. Thus, the left half and the right half of the abscissa correspond to the low and high initial NO concentrations, respectively. The first and third quarters have the low initial NO_2 concentration while the second and fourth quarters have the high one, and so on. The locations for the low- and high-ozone initial conditions are self-evident from the O_3 plots of the figures. Each plot in the figures contains two lines: a dashed line connecting the solutions from the exact solver and a solid line connecting the solutions of a given solver. The scales on the ordinate are based on the exact solutions. Therefore, predicted concentrations may exceed the scales.

Under daytime conditions, solutions from IEH37 and IEH26 agree very well with the exact solutions for all species under the given initial conditions. Hybrid + SS is less accurate especially under the high NO–low NO_2–low O_3 initial conditions where the |RE| for many species concentrations can be up to 0.2 (up to 1.0 in the case of PNA when negative concentrations are reset to zero). But these slight reductions in accuracy are notable only in OH, ROR, and TO_2 where the exact concentrations for the corresponding initial conditions are not near zero. Also, an overestimate of XO_2N occurs under the low NO–low NO_2–high O_3–low OLE initial conditions, with an |RE| of up to 0.3. UAM is somewhat less accurate than Hybrid + SS. Species solutions are generally within 0.1 of the exact solutions. As in Hybrid + SS, UAM overestimates XO_2N under similar conditions. UAM also tends to underestimate HNO_3, H_2O_2, PAN, and CRES, with an |RE| between 0.1 and 0.3 under the high O_3 initial conditions.

QSSA underestimates NO by about 40% under the low O_3 initial conditions. Inaccuracies of QSSA over a wide range of initial conditions are also evident for NO_2 (Figure 1a). The inaccuracies are the most serious under the high NO–low NO_2–low O_3 initial conditions. The solutions for O_3 are generally accurate except for QSSA. Overestimates are frequently seen (Figure 1b), with the largest occurring under the initial conditions of high NO–low NO_2–high O_3. For HNO_3, all solvers perform well except QSSA, QSSA + SS, and Hybrid (Figure 1c). Substantial underestimates occur over a wide range of initial conditions for QSSA + SS and Hybrid. QSSA, on the other hand, greatly overestimates HNO_3, by a factor of 2–15 (the latter occurring under the high NO–low NO_2–low O_3 initial conditions). The solutions for H_2O_2 are again poor for QSSA, QSSA + SS, and Hybrid (Figure 1d). Both QSSA and Hybrid yield very low concentrations (but nonconstant, around 1×10^{-5} ppm, which is the initial value for H_2O_2). In fact, the solutions practically do not respond to the variation of initial conditions of other species. QSSA + SS and hybrid, and in most cases, QSSA as well, substantially underestimate PAN (Figure 1e). For Hybrid, the |RE|s typically approach 1.0 but lower (0.7–0.8) under the high NO–low O_3 initial conditions. QSSA overestimates CRES (Figure 1f) (and CRO) significantly, especially under high initial TOL. The |RE|s typically range from 1 to 6. QSSA + SS and Hybrid, on the other hand, tend

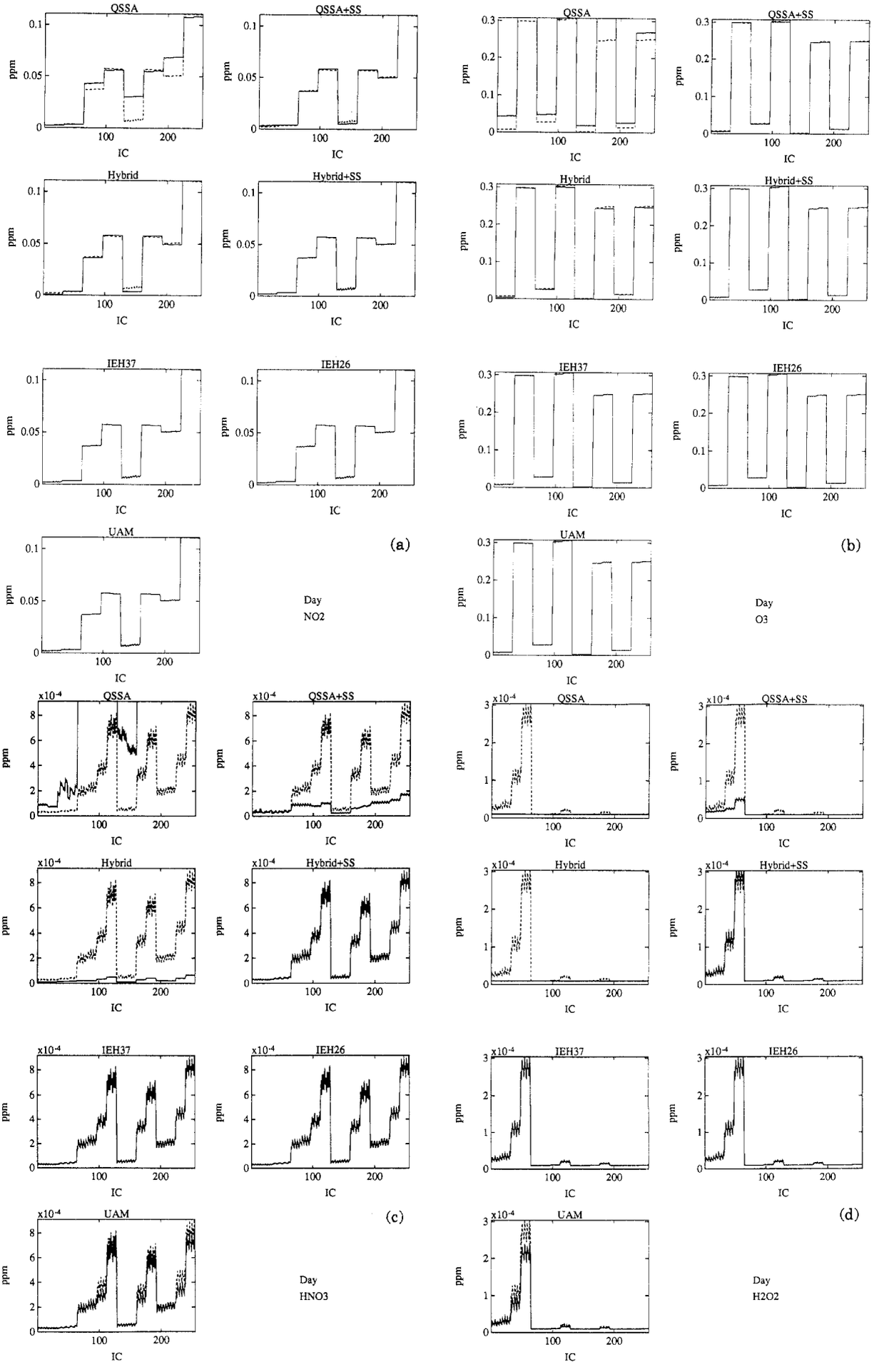

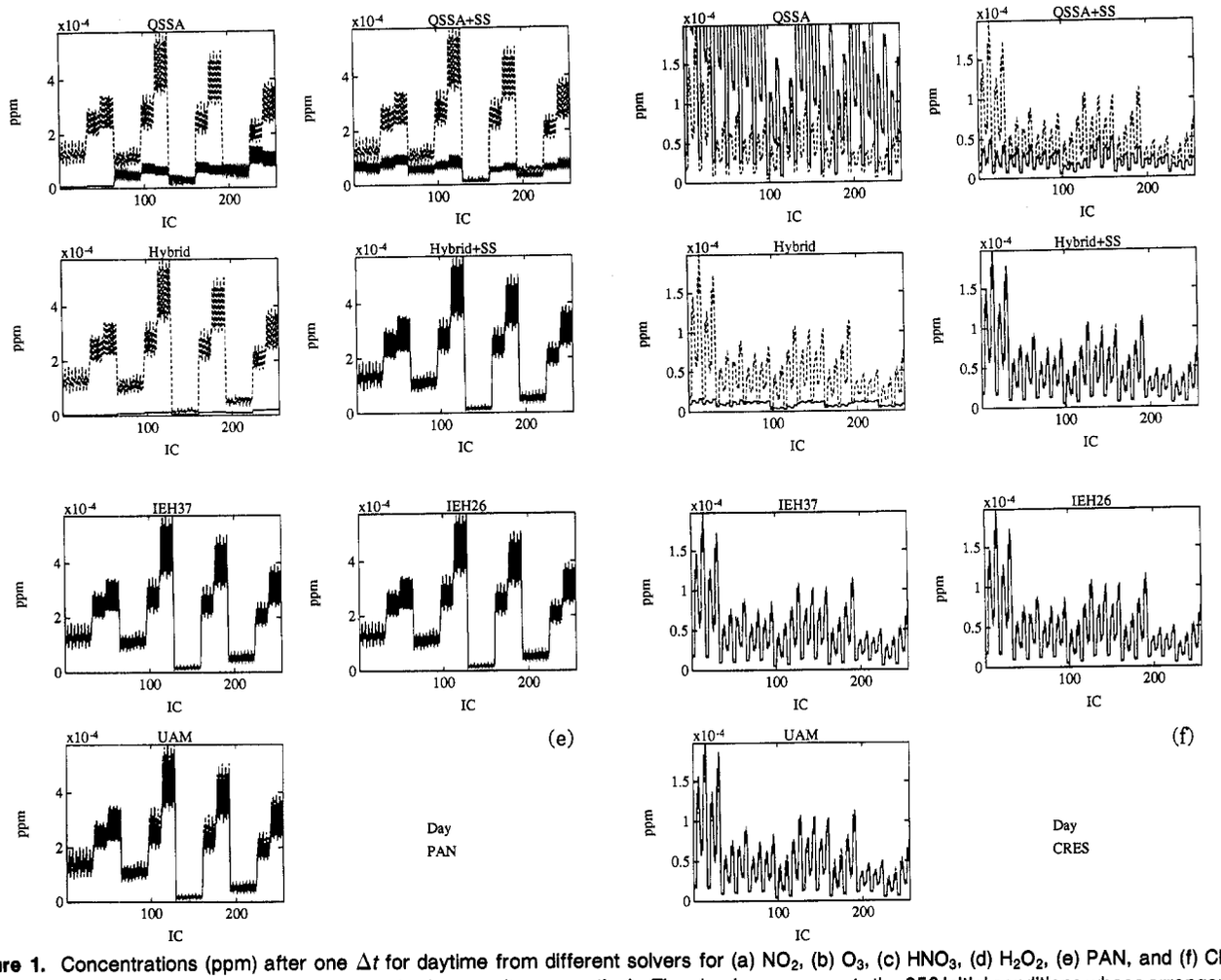

Figure 1. Concentrations (ppm) after one Δt for daytime from different solvers for (a) NO_2, (b) O_3, (c) HNO_3, (d) H_2O_2, (e) PAN, and (f) CRES. The dashed and solid lines represent the exact and solver results, respectively. The abscissa represents the 256 initial conditions whose arrangement is akin to an increasing eight-digit binary number with the left to right order of the digit being identical to the top to bottom order of the eight species with two concentration levels in Table 1.

to underestimate CRES (and CRO). The |RE|s are generally less than 0.8. Not shown in the figure is FORM. It is overestimated by QSSA by a factor of up to 2.

Under nighttime conditions, the NO concentrations, both exact and calculated, are high only under the high NO–low O_3 initial conditions. Under these conditions, QSSA underestimates NO substantially, by about 80%. QSSA also overestimates NO_2 (Figure 2a) by a factor of about 10 under the high NO–low NO_2–low O_3 initial conditions. O_3 is calculated quite accurately by the solvers except QSSA (Figure 2b). NO_3 is accurately calculated only by the IEH solvers (Figure 2c). Inaccuracy is significant for QSSA, QSSA + SS, and, to a lesser degree, Hybrid + SS and UAM, all under the high O_3 initial conditions unless both NO and NO_2 initial concentrations are also low. QSSA + SS and UAM substantially overestimate NO_3 under the high NO–low O_3 initial conditions. For HO_2, OH, ROR, C_2O_3, XO_2, and XO_2N, the accuracy of the solvers depends strongly on the initial concentrations of FORM under low initial O_3. Except for IEH, the |RE|s for these species concentrations tend to be large (e.g., up to 4 for HO_2, OH, XO_2, and XO_2N and up to 5000 for ROR in the case of UAM, all under the high NO–high NO_2–low O_3–low FORM conditions). HONO tends to be underestimated by non-IEH solvers (except QSSA which yields a large overestimate) by 20–40% under the high NO–low O_3–low FORM initial conditions. Inaccuracy in HNO_3 is significant for all non-IEH solvers (Figure 2d). The errors tend to occur when initial O_3 is low (except at low NO and low NO_2). The solvers are accurate for H_2O_2 under low initial O_3 but inaccurate (except the IEH solvers) under high initial O_3 (Figure 2e). For the latter, substantial underestimation is seen in QSSA, QSSA + SS, and Hybrid. PAN is also poorly calculated by non-IEH solvers. The errors are sensitive to initial FORM under low initial O_3. Hybrid, Hybrid + SS and UAM tend to underestimate PAN by 20–80% while QSSA and QSSA + SS tend to overestimate it, especially under high initial NO (by up to 700% and 80%, respectively). Solutions for CRES are generally not accurate except those from IEH37. Figure 2f shows the difficulty in reproducing the exact results. Most solvers do well for cases with vanishing solutions (associated with high O_3 initial conditions except when NO and NO_2 are also low) but not well for others. The IEH solvers reproduce the nonvanishing solutions very accurately, but IEH26 overestimates the vanishing solutions. In these cases, errors are introduced when small negative concentrations appear during the time integration and are reset to zero. In UAM, the concentrations are simply set to a small number (10^{-6} ppm) at the end of the integration. The solutions for solvers using the UAM steady-state algorithm are essentially constant at 10^{-5} ppm for the low NO–low O_3 initial conditions and are not responsive to the variation of the initial concentrations of XYL, as they should. For CRO, the IEH solvers have inaccuracies under high initial O_3 except when initial NO

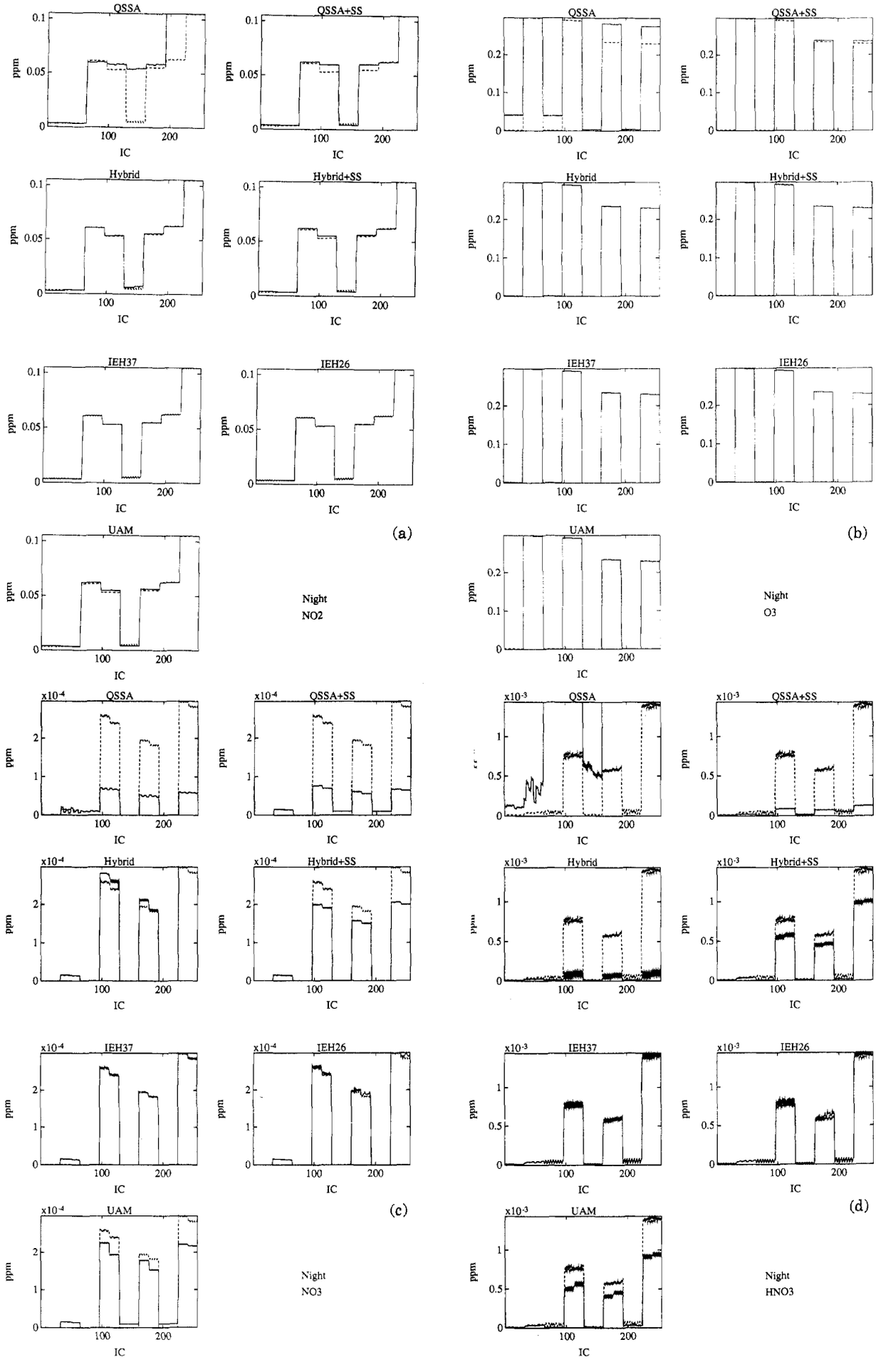

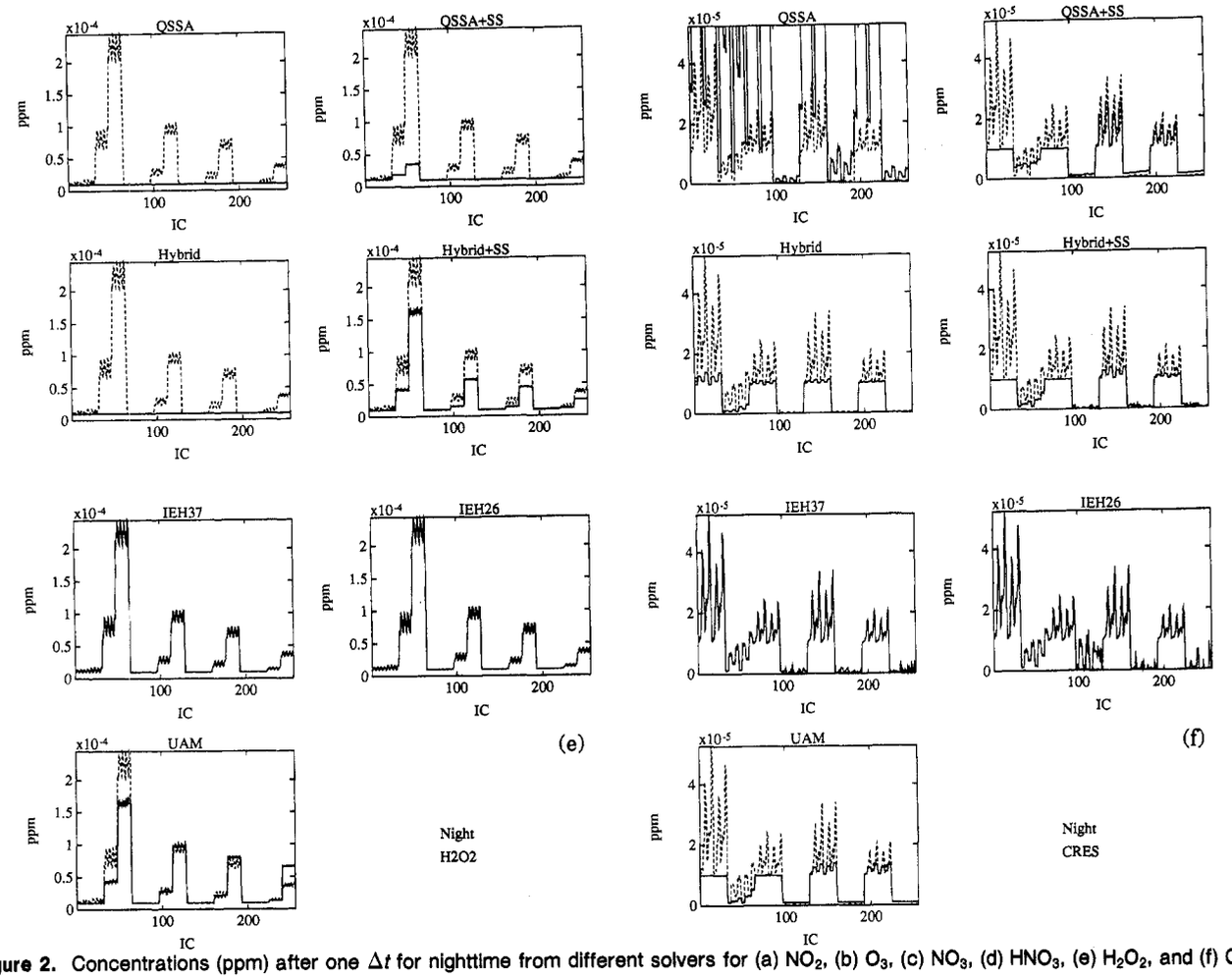

Figure 2. Concentrations (ppm) after one Δt for nighttime from different solvers for (a) NO_2, (b) O_3, (c) NO_3, (d) HNO_3, (e) H_2O_2, and (f) CRES. See Figure 1 for more detail.

and NO_2 are also low; other solvers are inaccurate under all high O_3 initial conditions.

Compared to all other solvers, the IEH conserves nitrogen the best. In terms of the av |RE| where the exact solution is the sum of the exact solutions of all nitrogen-containing species ($NO + NO_2 + NO_3 + 2N_2O_5 + PNA + PAN + HNO_3 + HONO$), IEH37 is the most accurate (5.1×10^{-5} for daytime, 1.4×10^{-4} for nighttime), followed by IEH26 (2.3×10^{-4}, 1.0×10^{-3}), Hybrid + SS (3.7×10^{-3}, 4.9×10^{-3}), UAM (3.9×10^{-3}, 7.4×10^{-3}), Hybrid (1.2×10^{-2}, 8.0×10^{-3}), QSSA (3.3×10^{-2}, 2.5×10^{-2}), and QSSA + SS (6.2×10^{-2}, 2.4×10^{-2}). In general, inaccuracy tends to be greater for high O_3 initial conditions. Most solvers attempt to rectify the lack of nitrogen mass balance by readjusting the concentrations of the nitrogen-containing species after each time step. The readjustment is generally *ad hoc* and may actually lead to a further deterioration of the solutions.

The computation time of a solver depends not only on the solution methodology but also on the initial conditions and the chemistry or mechanism involved (e.g., daytime vs nighttime). Whether the solver code exploits the unique capability of a computer also makes a difference. The codes we used are generic. Table 6 shows the CPU time for advancing the concentrations by one Δt per initial condition by each solver. The solvers were run on a Kubota Pacific Titan 3000 computer. Obviously, on average, both QSSA and QSSA + SS are 10 times or more faster than other solvers. Hybrid + SS is comparable to IEH26, both being faster than IEH37 and Hybrid on average over the 256 initial conditions. For daytime simulations, Hybrid + SS is slightly faster than IEH26 (0.025 s vs 0.03 s) under low initial O_3, but slightly slower (0.04 s vs 0.035 s) under high initial O_3. Hybrid is significantly slower except under the low NO–low NO_2–low O_3 initial conditions (0.025 s). For nighttime simulations, Hybrid + SS is faster than IEH26 (0.015 s vs 0.03 s) under low initial O_3 but is comparable to or considerably slower than IEH26 (which takes 0.05 s) under high initial O_3. Hybrid is about 20–30% faster than IEH26 under the low NO–low NO_2 (regardless of the O_3 level) initial conditions but is comparable to IEH26 under other low O_3 initial conditions and much slower (0.15 s) under other high O_3 initial conditions. UAM is by far the most time consuming for

Table 6. CPU Time (s) for Advancing Concentrations by One Δt (6 min) per Initial Condition

	daytime			nighttime		
solver	min	max	av	min	max	av
QSSA	<0.01	0.02	0.006	<0.01	0.02	0.006
QSSA + SS	<0.01	0.02	0.003	<0.01	0.02	0.004
Hybrid	0.02	0.19	0.082	<0.01	0.21	0.078
Hybrid + SS	0.01	0.10	0.036	<0.01	0.18	0.041
IEH37	0.04	0.06	0.051	0.04	0.09	0.057
IEH26	0.03	0.04	0.033	0.03	0.07	0.042
IEH26SS[a]	0.02	0.04	0.029	<0.01	0.05	0.026
UAM	0.07	0.58	0.160	0.01	4.67	1.226

[a] Initial concentrations of UAM steady-state species set at 10^{-16} ppm.

daytime simulations, but the computation time covers a very wide range and is very sensitive to the initial conditions for nighttime simulations. In fact, the computation time for UAM is very short under high initial O_3 but very much longer under low initial O_3. This is especially true when the NO initial concentrations are also high. In those cases, the computation time under low initial O_3 is about 400 times longer than that under high initial O_3! IEH has the least variability in computation time among the solvers tested. In contrast to UAM, it requires a shorter computation time under low initial O_3 than under high initial O_3. The ratios of high-to-low computation times are smaller for daytime simulations than for nighttime simulations (see above).

The UAM, QSSA + SS, and Hybrid + SS solvers do not require the input of the steady-state species concentrations whereas the solvers without the UAM steady-state assumptions require them. For IEH26, reducing the initial concentrations of the steady-state species to 10^{-16} ppm coupled with the 256 initial conditions does not alter the resulting concentrations of all species significantly. However, the computation time actually declines: the minimum, maximum, and average computation times to advance the solutions by one Δt are now 0.02, 0.04, and 0.029 s, respectively, for daytime and <0.01, 0.05, and 0.026 s, respectively, for nighttime (see Table 4). The decrease in computation time for nighttime is especially significant. It is typically 0.01 s (low NO) to 0.02 s (high NO) for the low O_3 initial conditions and 0.03–0.04 s for high O_3 initial conditions.

It should be noted that the UAM solver is very sensitive to not only the initial conditions but also the rate constants of certain reactions. In addition, this sensitivity changes with the platform used. For example, by setting the rates of formation and destruction of PNA to zero, as is done in the current version of the full UAM code (but not in the CB4 chemistry used in the single-cell trajectory model), the UAM solver becomes faster, by a factor of 3.5 (based on the average over the 256 initial conditions) for daytime simulations and unchanged for nighttime simulations on the Titan computer, but by a factor of 2.8 for daytime simulations and a factor of 29 for nighttime simulations on the Silicon Graphics Challenge computer. This gain in speed allows the full UAM to run faster than UAM coupled with the IEH solver. But if the rate constants for PNA are set to their original values, then the full UAM runs considerably slower, especially for nighttime. In fact, the UAM run fails to converge. Failure to converge in the full UAM runs often occurs; whereas replacing the UAM solver with IEH26 reduces such occurrences dramatically. This result will be reported elsewhere.

Because the computation time of the solver is sensitive to the initial conditions, whether a solver may be fast or slow in actual air quality modeling depends not only on how the solver is integrated in the model code but also on how different initial conditions are distributed among the grid cells and how this distribution changes with time. However, one may reasonably expect the QSSA and QSSA + SS solvers to be the fastest. IEH26 is expected to be comparable in speed to Hybrid + SS for both daytime and nighttime if very low initial concentrations are used for the steady-state species. As mentioned above, UAM is faster than IEH26 with PNA turned off, but slower and, in fact, failed in our test case when PNA is turned on.

Conclusion

The solvers were compared under a wide range of conditions, many of which may not be readily observed in the ambient atmosphere. However, because the accuracy and execution time of a solver strongly depend on the chemical system and the associated initial conditions, it is necessary that such comparison be done so that a fast solver that is accurate under a wide range of conditions may be identified.

In terms of accuracy, there is no doubt that the IEH solvers are the most accurate among the solvers studied while the QSSA, QSSA + SS, and Hybrid solvers are the least accurate. In terms of computation time, QSSA and QSSA + SS are by far the fastest. UAM is slow unless the rates of formation and destruction of PNA are set to zero. Both IEH26 and Hybrid + SS are fast while the former is more accurate under all tested conditions and conserves nitrogen mass. The IEH solver is also applicable to other stiff chemical systems. Accordingly, IEH26 should be an excellent choice as a fast and accurate chemistry solver in air quality modeling, combustion, and other reactive flow systems.

Literature Cited

(1) Hindmarsh, A. C., LSODE and LSODI, Two new initial value ordinary differential equation solvers. *ACM-SIGNUM Newsl.* **1980**, *15* (4), 10–11.

(2) Hesstvedt, E., Ø. Hov and I. S. A. Isaksen, Quasi-steady-state approximations in air quality modeling. *Int. J. Chem. Kinet.* **1978**, *10*, 971–994.

(3) Young, T. R.; Boris, J. P. A numerical technique for solving stiff ordinary differential equations associated with the chemical kinetics of reactive flow problems. *J. Phys. Chem.* **1977**, *81*, 2424–2427.

(4) U.S. EPA. *Urban Airshed Model Version 6.20, Dated 920825*; U.S. EPA: Research Triangle Park, NC, 1993.

(5) Sun, P.; Chock, D. P.; Winkler, S. L. An implicit–explicit hybrid solver for a system of stiff kinetic equations. *J. Comp. Phys.*, in press.

(6) Odman, M. T.; Kumar, N.; Russell, A. G. A comparison of fast chemical kinetic solvers for air quality modeling. *Atmos. Environ.* **1992**, *26A*, 1783–1789.

(7) Shieh, D. S.; Chang, Y.; Carmichael, G. R. The evaluation of numerical techniques for solution of stiff ordinary differential equations arising from chemical kinetic problems. *Environ. Software* **1988**, *3*, 28–38.

(8) Morris, R. E.; Myers, T. C. *User's Guide for the Urban Airshed Model, Vol. I: User's Manual for UAM(CB-IV)*; EPA-450/4-90-007A; U.S. EPA: Research Triangle Park, NC, June 1990.

(9) Milford, J. B.; Gao, D.; Russell, A. G.; McRae, G. J. Use of sensitivity analysis to compare chemical mechanisms for air-quality modeling. *Environ. Sci. Technol.* **1992**, *26*, 1179–1189.

(10) Yamartino, R. J.; Scire, J. S.; Hanna, S. R.; Carmichael, G. R.; Chang, Y. S. *CALGRID: A Mesoscale Photochemical Grid Model*; Report No. A049-1; California Air Resources Board: Sacramento, CA, June, 1989.

(11) McRae, G. J.; Russell, A. G.; Harley, R. A. *CIT Photochemical Airshed Model—Systems Manual*; Feb 1992; Available from Coordinating Research Council, 219 Perimeter Center Parkway, Atlanta, GA 30346.

Received for review January 19, 1994. Accepted June 29, 1994.®

® Abstract published in *Advance ACS Abstracts,* August 1, 1994.